World Journal of Engineering Research
Print ISSN: 2959-9865
Online ISSN: 2959-9873
DOI: https://doi.org/10.61784/wjer3084

A FINITE-ELEMENT-BASED PRESSURE ALLOCATION STRATEGY BETWEEN SEALANT AND MEMBRANE ELECTRODE IN PEM FUEL CELL STACKS

QiXin Liang[1], XinFeng Zhang[2*]
[1]*College of Automotive and Energy Engineering, Tongji University, Shanghai 201804, China.*
[2]*School of information and electrical engineering, Hangzhou City University, Hangzhou 310009, Zhejiang, China.*
[*]*Corresponding Author: XinFeng Zhang*

Abstract: Sealing reliability is essential to the safe and efficient operation of proton exchange membrane fuel cell (PEMFC) stacks. In practical stack assembly, however, increasing the seal compression to improve gas tightness may simultaneously raise the mechanical stress in the membrane electrode assembly (MEA), especially in the membrane and gas diffusion layer region. This trade-off makes conventional seal design based solely on leakage prevention insufficient for high-performance stack packaging. In this study, a finite-element-based pressure allocation strategy is developed to coordinate the mechanical requirements of the sealant and the MEA. A two-level modeling framework is adopted. First, a local metal bipolar plate-sealant-MEA frame model is established to verify sealing feasibility and evaluate the force requirement of the seal line under different compression ratios. Then, a refined full model including the flow-field ribs, seal groove, sealant, proton exchange membrane, frame region, and gas diffusion layer is built to investigate the coupling between seal compression, bipolar-plate displacement, and membrane stress. The results show that although a semicircular sealant can satisfy the sealing criterion in the local model, it becomes unsuitable in the full structure because the compression required to ensure gas tightness leads to excessive membrane stress. Under a 20% compression ratio, the maximum equivalent stress in the proton exchange membrane reaches approximately 4.8 MPa, which is far above the desired level of about 1.4 MPa. An improved pressure allocation strategy is therefore proposed by controlling bipolar-plate displacement rather than directly preserving the seal compression state. Based on this strategy, an optimized rectangular sealant section at a compression ratio of 17% achieves both adequate gas tightness and acceptable membrane stress. The study provides a practical finite-element-guided route for coordinated seal and MEA design in PEMFC stacks.
Keywords: Proton exchange membrane fuel cell; Sealant; Membrane electrode assembly; Pressure allocation; Finite element analysis

1 INTRODUCTION

PEMFCs have been widely regarded as one of the most promising power sources for next-generation transportation systems because of their high efficiency, high power density, low operating temperature, and fast start-up capability [1]. In a practical PEMFC stack, however, electrochemical performance and structural reliability are strongly coupled with the assembly condition. Among the key structural components, the sealing system is particularly critical because it must prevent reactant leakage, maintain electrical insulation between adjacent cells, and ensure proper contact pressure distribution among internal components [2-3].

The sealant in a PEMFC stack does not function as an isolated gasket. Its compression behavior directly affects the deformation of the bipolar plate, the contact state of the gas diffusion layer (GDL), and the stress distribution in MEA. A higher packaging load may improve sealing reliability and reduce interfacial contact resistance, but excessive compression can also over-compress the GDL, reduce its porosity, and thus impair mass transport and fuel-cell performance [1]. Therefore, seal design in PEMFC stacks is essentially a coupled mechanical problem, rather than a simple leakage-prevention problem.

Extensive efforts have been devoted to understanding the mechanical response of PEMFC stacks under assembly load. Alizadeh et al. established a two-dimensional finite element model, and verified it using a three-dimensional model and pressure-sensitive-film experiments, showing that parameters such as endplate thickness, material, seal stiffness, stack size, and cell position significantly affect the contact pressure distribution over the active area [4]. Jia et al. developed a three-dimensional thermo-mechanical assembly model and demonstrated that thermal coupling has a significant influence on the stress distribution in the MEA and among individual cells [5]. Zhang et al further analyzed a multistage three-dimensional steady thermo-mechanical PEMFC model and reported that the surface contact pressure of the MEA tends to become more uniform after thermal stabilization [6]. Qiu et al. investigated the thermo-mechanical behavior of the MEA under cyclic temperature conditions and showed that membrane fatigue failure may occur under coupled thermal and humidity variations [7].

In parallel with stack-level mechanical studies, increasing attention has been paid to the material behavior and structural design of PEMFC sealants. Kumar et al. reviewed the physical and chemical properties required for PEMFC sealants and emphasized the importance of material stability under acidic, humid, and temperature-varying environments [2].

Cui et al. investigated the stress-relaxation behavior of liquid silicone rubber seals, highlighting the time-dependent mechanical characteristics that must be considered in durability-oriented design [3]. Qiu et al. studied the pressure distribution in a single cell under clamping load through both finite element simulation and experiments, and explained the origin of pressure nonuniformity caused by component warpage [8]. Carral and Mélé developed a three-dimensional finite element model to analyze PEMFC stack assembly and showed that the number and position of cells influence MEA compression force, contact pressure, and porosity distribution [9].

Recent studies have further explored seal-section geometry and efficient modeling methods. Zhao et al. established finite element models based on the Mooney-Rivlin hyperelastic constitutive law and analyzed the uniformity of sealant contact pressure in PEMFC stacks [10]. Jiang et al compared semicircular, rectangular, double-peak, and triple-peak seal sections under different temperatures and compression ratios, and proposed a triple-peak structure with improved sealing reliability [11]. Zhou performed experimental characterization of sealant hyperelasticity and optimized the geometry and dimensions of the triple-peak section to improve contact-pressure distribution [12]. In addition, equivalent-stiffness-based methods have been proposed to predict contact pressure rapidly with acceptable accuracy, and flow-field structural studies have provided useful guidance for bipolar-plate and stack design [10-11].

Although these studies have substantially advanced the understanding of stack assembly mechanics and seal behavior, most existing work still focuses primarily on either contact-pressure distribution or sealing reliability alone. Comparatively limited attention has been paid to the coordinated design problem between seal compression and MEA mechanical safety. In practice, a seal geometry that appears acceptable in a simplified local model may still induce excessive membrane stress when the flow-field ribs, bipolar-plate deformation, and full layered structure of the MEA are taken into account. Therefore, a design framework that simultaneously considers gas tightness and membrane-safe stress levels remains necessary.

To address this issue, this study develops a finite-element-based pressure allocation strategy between the sealant and the membrane electrode in a PEMFC stack. A local bipolar plate-sealant-MEA frame model is first established to verify the basic sealing feasibility of the seal section. A refined full model including the seal groove, flow-field ribs, GDL, and membrane is then constructed to evaluate the coupling among seal compression, bipolar-plate displacement, and membrane stress. Based on these analyses, an optimized seal-section design and a displacement-compatible pressure allocation strategy are proposed to balance gas-tight sealing performance and MEA mechanical safety.

2 MODELING STRATEGY AND FINITE ELEMENT METHOD

2.1 Design Objective and Sealing Criterion

The essential function of the sealant is to maintain a gas-tight cavity formed by the membrane electrode assembly, the bipolar plate, and the sealing structure. Under the internal gas pressure, the sealant tends to move outward. To prevent this movement and maintain sealing reliability, the resistance provided by friction at the contact interfaces must be sufficiently large.

Based on the mechanical equilibrium of the sealing interface, the sealing condition can be written as

$$\mu\delta S_2 \geq P S_1 \tag{1}$$

where μ is the friction coefficient between the sealant and the contact surface, δ is the normal contact pressure, S_2 is the sealing contact area after compression, P is the working gas pressure, and S_1 is the area exposed to the working medium. For the two-dimensional cross-sectional analysis adopted in this study, as presented in Figure 1, Eq. (1) can be simplified as

$$\mu\delta L \geq P\mathrm{h}_1 \tag{2}$$

where L is the contact width between the compressed sealant and the bipolar plate, and h_1 is the sealant height after compression. This criterion provides the fundamental basis for determining whether a given seal geometry and compression level can prevent leakage.

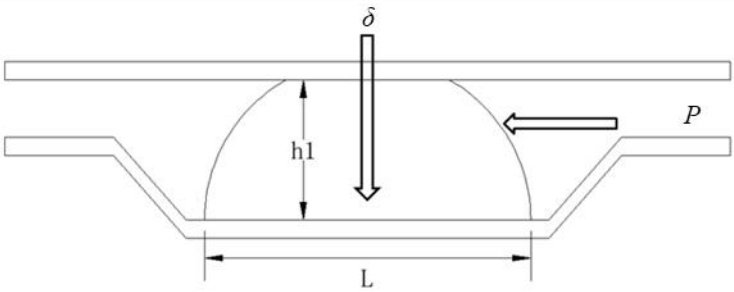

Figure 1 Schematic Diagram of the Sealing Model

The purpose of the present work is not merely to maximize the left-hand side of Eq. (2). Instead, the target is to satisfy the sealing condition while avoiding excessive stress transfer to the membrane electrode region. Accordingly, the design problem is formulated as a pressure allocation problem between the sealant and the MEA. In practical terms, the sealant

must be compressed enough to ensure gas tightness, but not so much that the induced deformation of the bipolar plate and gas diffusion layer drives the membrane stress beyond the desired limit.

2.2 Hyperelastic Constitutive Model

Sealants in PEMFC stacks are usually made of rubber-like materials and undergo large elastic deformation during assembly. Their mechanical response is nonlinear, nearly incompressible, and substantially different from that of ordinary linear elastic solids. For this reason, a hyperelastic constitutive law is adopted in the present study. Among the available models, the Mooney-Rivlin formulation is used because it is well suited to the finite element description of large-deformation elastomers in engineering applications.

The strain-energy density function of the classical Mooney-Rivlin model can be expressed in terms of the strain invariants. In this work, a three-parameter Mooney-Rivlin model is used for the sealant material in order to capture nonlinear deformation behavior more reasonably than a linear or overly simplified elastic model. The material parameters used for the local model are C_{10}=0.366 MPa, C_{01}=0.011 MPa, and C_{11}=0.284 MPa. The choice of a hyperelastic model is important because seal behavior under compression is governed not only by the final displacement but also by the way the material redistributes contact pressure along the interface.

2.3 Local Model

A local symmetric model is first established to evaluate the basic sealing capability of the sealant, as shown in Figure 2.

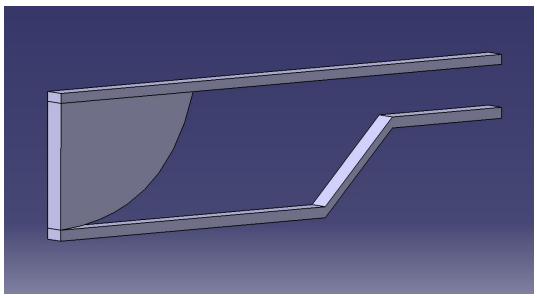

Figure 2 Local Symmetric Finite Element Model of the Bipolar Plate-Sealant-MEA Frame Structure

The model consists of a metal bipolar plate, a sealant, and the MEA frame region. The MEA thickness is set to 0.09 mm. The sealant width is 3 mm, its thickness is 1.15 mm, and its initial cross-section is semicircular. The metal bipolar plate thickness is 0.1 mm, while the seal groove width and depth are 6 mm and 0.76 mm, respectively. To facilitate numerical implementation, the components are extruded into thin three-dimensional bodies with an extrusion height of 2 mm. The contact between the MEA frame and the sealant is defined as no-separation contact, while the contact between the sealant and the bipolar plate is defined as frictional contact with a friction coefficient of 0.068. Material parameters used in the local model are shown in Table 1.

Table 1 Material Parameters Used in the Local Model

Component	Parameter	Value
Metal BPP	Elastic modulus (GPa)	158
	Poisson's ratio	0.3
	Yield strength (MPa)	312
MEA frame region	Elastic modulus (N/mm²)	6080
	Poisson's ratio	0.33
	Density (g/cm³)	1.36

Because the model is geometrically symmetric, a symmetry constraint is imposed along the middle plane to reduce computational cost. The lateral sides of the thin bodies are supported to mimic the constraint from adjacent stack regions. The bottom of the bipolar plate is fixed, and a prescribed downward displacement is applied to the top of the MEA to represent different seal compression ratios. Large deformation is enabled in the finite element solution. Three nominal compression ratios are investigated: 15%, 20%, and 25%. These correspond to displacements of 0.1725 mm, 0.23 mm, and 0.2875 mm, respectively.

The local model serves as a preliminary screening tool. It is useful for verifying whether a given seal section can satisfy the sealing criterion and for estimating the evolution of interface contact pressure with compression. However, it does not include the flow-field ribs, the active-area support condition, or the detailed layer-wise structure of the MEA. Therefore, its conclusions must be validated by a more refined model before a final design decision is made.

2.4 Refined Full Model and Evaluation Procedure

To investigate the coupling between seal compression and the stress state of the active region, a refined full model is constructed as shown in Figure 3. In this model, the bipolar plate includes the seal groove and several flow-field ribs adjacent to the sealing region. The groove geometry follows a practical design specification. The groove bottom width is 2.0 mm, the groove opening width is 2.8 mm, and the groove depth is 0.40 mm. The flow-field channel is modeled using a square channel configuration. The bipolar plate wall thickness is 0.1 mm, the rib width is 1 mm, the channel height is 0.6 mm, the corner radius is 0.15 mm, and the side-wall angle is 90° .

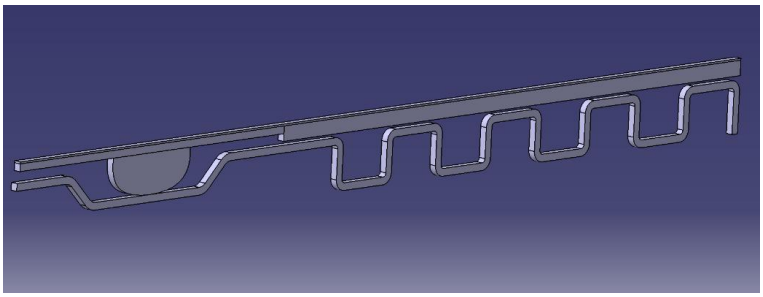

Figure 3 Refined Full Model Including the Seal Groove, Flow-Field Ribs, Membrane, Frame Region, and Gas Diffusion Layer

Unlike the local model, the MEA is refined into multiple parts according to actual structural composition. The central proton exchange membrane is assigned a thickness of 0.05 mm, the frame region in contact with the sealant has a thickness of 0.1 mm, and the gas diffusion layer in contact with the bipolar plate has a thickness of 0.2 mm. A gap of 0.05 mm is reserved initially between the bipolar plate and the gas diffusion layer. This refined representation allows the model to capture the transmission of mechanical load from the sealant and bipolar plate into the membrane region more realistically.

The full-model evaluation procedure is as follows. First, a seal geometry is assigned and compressed to a prescribed nominal ratio. Then, the resulting deformation, contact pressure, and membrane equivalent stress are examined. If the sealing condition is satisfied but the membrane stress exceeds the desired limit, the strategy is revised. In particular, instead of preserving the compressed seal height alone, the displacement of the bipolar plate is controlled so that the compression imposed on the gas diffusion layer and the membrane remains within a reasonable range. Through this procedure, the seal geometry and thickness are iteratively adjusted until both sealing reliability and membrane stress requirements are met.

3 RESULTS AND DISCUSSION

3.1 Local-Model Verification of Sealing Feasibility

The first set of simulations is performed on the local model with the semicircular sealant section. The deformation pattern is symmetric with respect to the model midplane, and the maximum deformation occurs near the outer lower side of the semicircular sealant. As the compression ratio increases, the contact pressure at the sealant-bipolar-plate interface rises markedly. The maximum contact pressures are 0.79 MPa, 1.14 MPa, and 1.68 MPa for compression ratios of 15%, 20%, and 25%, respectively, as shown in Figure 4. This trend is consistent with the basic expectation that a larger prescribed displacement produces a higher interface pressure and thus a stronger sealing tendency.

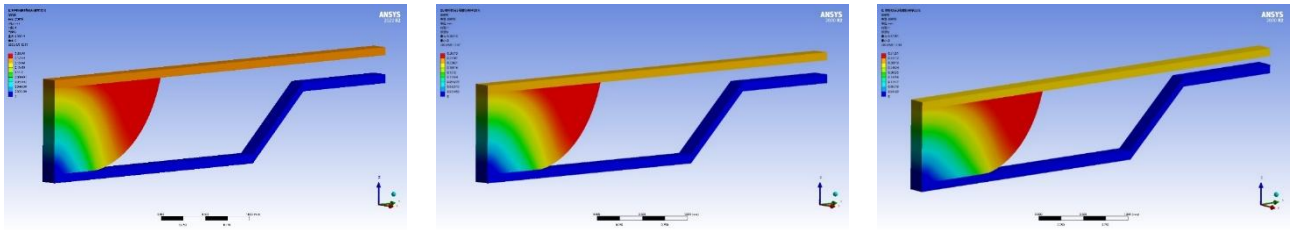

(a) (b) (c)

Figure 4 Displacement Contours of the Semicircular Sealant in the Local Model under 15%(a), 20%(b), and 25%(c) Compression Ratios

Comparison of local-model results for different compression ratios, including prescribed displacement, maximum contact pressure, and sealing assessment are shown in Table 2. When the sealing criterion in Eq. (2) is checked, all three compression ratios satisfy the gas-tightness requirement in the local model. This result indicates that the semicircular sealant section has sufficient sealing potential under the simplified support condition. Nevertheless, the margin is not equally robust in all cases. At 15% compression, the sealing condition is met only slightly above the threshold, which

means that the design may be sensitive to manufacturing tolerance, surface roughness, or assembly variation. By contrast, the 20% and 25% cases provide a larger sealing margin.

Table 2 Comparison of Local-Model Results for Different Compression Ratios

Compression ratio (%)	Prescribed displacement (mm)	Maximum contact pressure (MPa)	Sealing assessment
15	0.1725	0.79	Satisfied (marginal)
20	0.2300	1.14	Satisfied
25	0.2875	1.68	Satisfied

From the standpoint of local sealing feasibility alone, one might conclude that a compression ratio of 20% or 25% is preferable because it offers higher contact pressure and stronger resistance against leakage. This is precisely the point at which a design based only on local criteria can become misleading. The local model does not reflect the influence of the flow-field ribs, the layered MEA structure, or the coupling between seal compression and bipolar-plate deformation. Therefore, the result of the local analysis should be interpreted as a necessary but not sufficient condition for final design acceptance.

The local-model results still provide two useful insights. First, they confirm that a semicircular sealant can be made gas-tight within a moderate compression range. Second, they show that increasing compression is an efficient but potentially dangerous way to improve sealing, because the method raises not only the sealing pressure but also the load transferred to the surrounding structure. These observations motivate the refined full-model analysis presented below.

3.2 Conflict Revealed by the Full Model

When the semicircular sealant is transferred from the local model to the refined full structure, the design behavior changes substantially. In the refined model, the seal no longer works against a purely simplified support condition. Instead, its deformation is coupled with the groove geometry, flow-field ribs, gas diffusion layer, and the membrane itself. As a result, the compression ratio required to ensure adequate sealing can no longer be judged only from the local section response.

The full-model simulations show that the original design strategy, which attempts to preserve the compressed sealant height while increasing compression, when necessary, leads to excessive stress in the membrane region. In the case of a 20% compression ratio, as shown in Figure 5, the maximum equivalent stress in the proton exchange membrane already reaches approximately 4.8 MPa. This value is far above the target level of about 1.4 MPa and indicates a high risk of mechanical overloading in the active area. Since the membrane stress becomes unacceptable at 20% compression, it is unnecessary to continue to 25% compression for the same geometry. A further increase in compression would be expected to aggravate the problem.

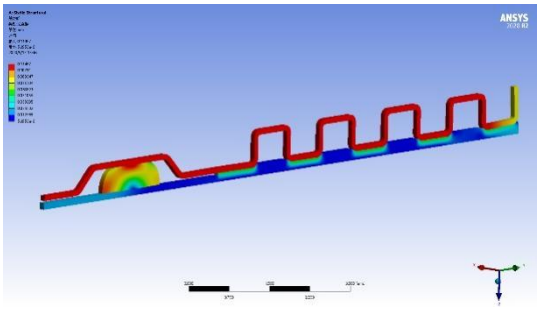

Figure 5 Displacement Contours of the Semicircular Sealant in Refined Full Structure under 20% Compression Ratios

This result reveals an important discrepancy between local and full-model evaluations. In the local model, higher compression appears favorable because it improves gas-tightness margins. In the full model, however, the same increase in compression causes excessive deformation transfer through the bipolar plate and gas diffusion layer, thereby pushing the membrane stress into an unsafe range. The discrepancy highlights that sealing feasibility and mechanical compatibility cannot be assessed independently when the stack structure is strongly coupled.

A closer examination suggests that the membrane stress is influenced mainly by the compression imposed on the gas diffusion layer and the displacement of the bipolar plate over the active region. Therefore, the original design logic should be revised. Rather than simply preserving the post-compression seal height or directly increasing the nominal seal compression, the more effective strategy is to control the bipolar-plate displacement. According to the simulation results, maintaining the single-side bipolar-plate displacement within approximately 0.08-0.10 mm, corresponding to a total displacement of 0.16-0.20 mm for the two sides, can keep the maximum membrane stress near the desired 1.4 MPa level.

This finding is significant from an engineering perspective. It means that the key control variable is not merely the nominal compression ratio of the sealant itself, but the overall deformation compatibility between the sealing groove,

seal section, bipolar plate, and MEA. Once this perspective is adopted, the sealant geometry can be redesigned to produce sufficient sealing pressure under a limited bipolar-plate displacement.

3.3 Pressure Allocation Strategy and Section Optimization

Guided by the full-model observations, the pressure allocation strategy is modified. The revised strategy can be summarized as follows: the mechanical demand of the MEA is first defined through an allowable membrane stress target, and the bipolar-plate displacement is limited accordingly; then the sealant geometry and thickness are adjusted so that the sealing criterion is met under this constrained deformation state. In other words, the design sequence is changed from a seal-compression-driven approach to a displacement-compatible and membrane-safe approach.

Under this revised strategy, the semicircular section is found to be intrinsically disadvantaged. Although it performs well in the local model, it tends to produce an unfavorable contact-pressure distribution in the full model. One reason is that the semicircular section develops a nonuniform interface pressure, typically higher in the central region and lower near the edges, which reduces the effective average sealing pressure. Another reason is that a larger compression is often needed for this section to satisfy the full-model sealing requirement, and such a larger compression amplifies the risk of stress concentration and excessive loading in adjacent layers.

To overcome this limitation, the sealant section is changed to a rectangular geometry. Under compression, the rectangular section expands primarily toward both sides, which increases the effective contact width and makes it easier to generate a higher average sealing pressure without excessively increasing membrane stress. The simulations confirm that this geometric modification is beneficial under the displacement-controlled design framework.

At a compression ratio of 17%, the rectangular sealant exhibits a markedly improved mechanical response. The maximum contact pressure at the sealant-bipolar-plate interface reaches about 0.907 MPa, demonstrating a stronger and more effective sealing contact than in the previous design. The processed interface data further show that the average contact pressure is approximately 0.5235 MPa. When substituted into the sealing criterion, the frictional sealing term exceeds the corresponding pressure-height term, indicating that the gas-tightness requirement is satisfied. More importantly, the maximum equivalent stress in the membrane near the gas-diffusion-layer contact region remains around 1.4 MPa, which matches the target level established for mechanical safety.

These results indicate that the rectangular section succeeds in achieving the two design objectives simultaneously: it generates sufficient sealing force to prevent leakage and, at the same time, avoids excessive stress transfer to the membrane. Compared with the semicircular design, the optimized rectangular section also requires a lower compression ratio than the full-model-feasible semicircular alternative would require, which implies a lower overall clamping demand for the packaging system, as shown in Figure 6.

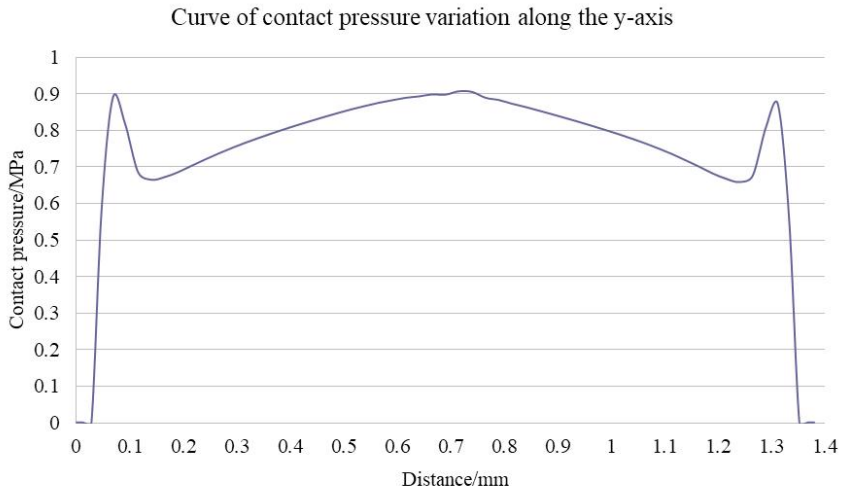

Figure 6 Contact-Pressure Distribution of the Optimized Rectangular Sealant at 17% Compression

The optimized result also clarifies the physical meaning of pressure allocation. The goal is not to maximize pressure in every part of the stack, but to distribute the available packaging load rationally. A properly designed sealant should consume enough load to ensure gas sealing while leaving the active region in a stress window compatible with electrochemical operation. The present finite-element procedure provides a direct way to realize this objective in practical structural design.

3.4 Engineering Implications

The results of this study provide several practical implications for PEMFC stack sealing design. First, a locally acceptable sealing solution cannot be assumed to be acceptable for the full stack structure. A local model is still valuable because it can quickly identify whether a candidate seal section has basic sealing potential, but it should not be

the sole basis for final structural decisions. The active-area response and layer-wise load transfer must be evaluated through a refined model.

Second, the membrane-safe design target can serve as an effective upper bound for seal optimization. In conventional practice, designers may start from seal compression and then check whether leakage is prevented. The present results suggest that it is often more effective to reverse the logic: define an allowable membrane stress level, translate it into a controlled bipolar-plate displacement, and then optimize the seal geometry to satisfy the sealing criterion under that constraint. This approach naturally embeds electrochemical considerations into the mechanical design process.

Third, seal section geometry deserves more attention than is sometimes assumed. Even when two seal sections are made of the same material and operate within a similar compression range, their pressure-distribution patterns can differ considerably. The comparison in this work shows that the rectangular section is better suited than the semicircular section to the present groove and layer configuration because it yields higher effective sealing pressure under a membrane-safe deformation state. This does not imply that the rectangular section is universally optimal for all PEMFC stacks, but it does demonstrate that section geometry must be selected together with groove shape, bipolar-plate stiffness, and MEA support conditions.

Finally, the proposed method can be extended beyond the present case. In future applications, additional factors such as temperature variation, long-term stress relaxation, manufacturing tolerance, and assembly misalignment can be incorporated into the same design framework. The essential principle will remain the same: sealing design should be treated as a coupled structural optimization problem rather than a single-parameter compression problem.

4 CONCLUSIONS

A finite-element-based study was conducted to develop a coordinated pressure allocation strategy between the sealant and the membrane electrode in a PEMFC stack. By combining a local sealing model with a refined full structural model, the relationship among seal compression, interface contact pressure, bipolar-plate displacement, and membrane stress was systematically clarified. The main conclusions are as follows.

First, the nonlinear large-deformation behavior of the sealant should be modeled using a hyperelastic constitutive law. Linear elasticity is inadequate for accurately describing the compression response of the rubber-like sealing material.

Second, a semicircular sealant section performs reasonably well in a simplified local model and can satisfy the gas-tightness criterion at compression ratios as low as 15%. However, this local success does not guarantee compatibility with the full stack structure. In the refined full model, a 20% compression ratio already drives the maximum membrane stress to about 4.8 MPa, far above the desired level, demonstrating that a design based solely on local sealing considerations may be mechanically unsafe.

Third, a displacement-compatible pressure allocation strategy is more suitable than a purely compression-driven strategy. By controlling bipolar-plate displacement and redesigning the seal section, a rectangular sealant with a compression ratio of 17% was found to achieve both reliable gas sealing and an acceptable membrane stress of approximately 1.4 MPa. This optimized design provides a practical route for balancing sealing reliability and MEA mechanical safety in PEMFC stack packaging.

Overall, the study shows that effective PEMFC seal design should be based on coordinated structural analysis rather than on leakage prevention alone. The proposed framework offers a useful basis for further optimization of stack sealing structures in future engineering applications.

COMPETING INTERESTS

The authors have no relevant financial or non-financial interests to disclose.

FUNDING

The project was supported by Zhejiang Province's "Sharp Sword +X" Key Science and Technology Program Project (2025C01146).

REFERENCES

[1] Agyekum E B, Ampah J D, Wilberforce T, et al. Research progress, trends, and current state of development on PEMFC-new insights from a bibliometric analysis and characteristics of two decades of research output. Membranes, 2022, 12(11): 1103.

[2] Kumar V, Koorata P K, Shinde U, et al. Review on physical and chemical properties of low and high-temperature polymer electrolyte membrane fuel cell (PEMFC) sealants. Polymer Degradation and Stability, 2022, 205: 110151.

[3] Cui T, Lin C, Chien C, et al. Service life estimation of liquid silicone rubber seals in polymer electrolyte membrane fuel cell environment. Journal of Power Sources, 2011, 196(3): 1216-1221.

[4] Alizadeh E, Momenifar M, et al. Investigation of contact pressure distribution over the active area of PEM fuel cell stack. International Journal of Hydrogen Energy, 2016, 41(4): 3062-3071.

[5] Jia F, Tian X, Zhang G, et al. Thermal and mechanical investigation of proton exchange membrane fuel cells under combined loading conditions. Applied Thermal Engineering, 2024, 241: 122448.

[6] Zhang Z, Zhang J, Shi L, et al. A Study of Contact Pressure with Thermo-Mechanical Coupled Action for a Full-Dimensional PEMFC Stack. Sustainability, 2022, 14(14): 8593.
[7] Qiu D, Peng L, Liang P, et al. Mechanical degradation of proton exchange membrane along the MEA frame in proton exchange membrane fuel cells. Energy, 2018, 165: 210-222.
[8] Qiu D, Yi P, Peng L, et al. Study on shape error effect of metallic bipolar plate on the GDL contact pressure distribution in proton exchange membrane fuel cell. International Journal of Hydrogen Energy, 2013, 38(16): 6762 -6772.
[9] Carral C, Mélé P. A numerical analysis of PEMFC stack assembly through a 3D finite element model. International Journal of Hydrogen Energy, 2014, 39(9): 4516-4530.
[10] Zhao J, Guo H, Wang Z, et al. Research on Design and Optimization of Large Metal Bipolar Plate Sealing for Proton Exchange Membrane Fuel Cells. Sustainability, 2023, 15(15): 12002.
[11] Jiang W, Zhang K, Huang X, et al. Influence of clamping pressure on contact pressure uniformity and electrical output performance of proton exchange membrane fuel cell. Applied Energy, 2024, 353: 122021.
[12] Zhou Z, Qiu D, Zhai S, et al. Investigation of the assembly for high-power proton exchange membrane fuel cell stacks through an efficient equivalent model. Applied Energy, 2020, 277: 115532.